

# DIRECTIVITY CONTROL USING A STRUCTURAL ACTUATOR ARRAY

Nikolaos Kournoutos and Jordan Cheer

*University of Southampton, Southampton, Hampshire, United Kingdom*

*email: nk1y17@soton.ac.uk*

Directional sound fields can be generated by arrays of multiple sound sources, with the most common and straightforward method being an array of loudspeaker drivers. Although such a system is capable of high levels of directivity control over a broad bandwidth and with good audio quality, it can be prohibitively expensive and too fragile in certain applications. This work presents and investigates the idea of using an array of actuators mounted to a structure to generate a directional sound field. Inertial actuators have previously been used as an affordable and robust alternative to conventional loudspeakers, particularly in applications where the actuators can be used to drive a structure that would already be in place to radiate the desired sound field and where the required audio quality is lower. By distributing a number of actuators on a structure, and controlling the relative amplitudes and phases with which they are driven, it is possible to manipulate the structural vibration such that it generates a controlled directional sound field. In this work, an analytical model is first formulated of a rectangular panel excited by an array of structural actuators, approximated as point forces acting perpendicularly to the surface of the panel. This model is used to perform a simulation based parametric study, which provides insights into the design trade-offs for a structural actuator array based system. In particular, this considers how the number of actuators, their geometry and the dimensions of the structure influence the directivity control and achievable bandwidth. Based on this parametric study, a structural actuator array is assembled using a rectangular aluminium panel and six actuators for testing and evaluation through measurements in an anechoic chamber.

Keywords: directivity control, inertial actuators

---

## 1. Introduction

Although the concept of control over the directivity of a sound field is not novel, technological developments in the recent years have brought forward new necessities and potential for implementations of such features in fields from personal entertainment systems [1] to automotive safety [2]. To achieve this, an array of multiple loudspeakers is the most straightforward approach taken. Other methods, such as the use of parametric arrays incorporating ultrasonic transducers have been suggested [3]. Such systems are capable of good performance and bandwidth. However, they could be liable to failure when exposed to a harsh environment and rough use that certain applications require, and are relatively expensive to manufacture and maintain for wide use. As a lower cost and increased durability alternative to these loudspeaker based systems, this paper will investigate a solution which instead uses inertial actuators.

A typical dynamic loudspeaker utilises a voice coil to drive a diaphragm that, through its vibration, radiates sound. The structural array consists of a number of inertial actuators acting upon a panel, which could be part of the structure that hosts the array like a ceiling panel in a room or the body of a car. As with a loudspeaker array, the interference effects from vibrations caused by multiple actuators will cause a directionally radiated sound field. One of the key differences between the two systems is that instead of multiple diaphragms being independent from each other, the vibration of the radiating panel at any one point is affected by the force applied by every actuator. Existing research on has already investigated the use of actuators as an alternative to a loudspeaker for audio reproduction, though results showed significant bandwidth limitations [4].

This paper presents an investigation of a structural actuator based directional acoustic array. An analytical mathematical model is first formulated which is used to simulate the system and estimate its radiated sound field. A parametric study is then performed to investigate the effect of actuator number and positioning, as well as the size of the panel on the overall performance. Finally, preliminary experimental results are presented.

## 2. Mathematical Model

Figure 1 illustrates the geometry and approximations considered for the mathematical model of the structural array. The plate is a thin rectangular panel of length  $a$ , height  $b$  and thickness  $h$ . The actuators have been approximated by single point forces acting perpendicularly to the  $ab$  plane. In practice an actuator will have finite dimensions, however, since the actuators would be small compared to the size of the panel considered in this application, this is a reasonable approach considering the computational simplicity that it offers. Another parameter not considered is the weight of each actuator, which would normally bear an effect on the structural response of the panel. Again, since the mass of the actuators is small compared to that of the plate, the model is expected to be sufficiently accurate.

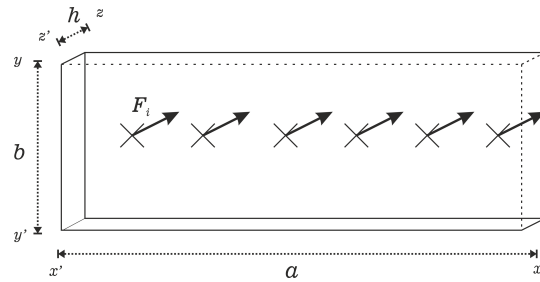


Figure 1: Schematic for the mathematical model of the structural array. A rectangular plate of thickness  $h$  is excited by a number of individual point forces  $F_i$  perpendicular to the plane defined by the length  $a$  and width  $b$  of the plate.

### 2.1 Vibration of a Simply Supported Thin Plate Excited by Point Forces

The operation of the structural array is based on the vibration of a rectangular thin plate which is simply supported along the edges, as presented in [5]. The equation of motion for such a plate, according to [6] is

$$\frac{h^3 E}{12(1 - \nu^2)} \left( \frac{\partial^4 w}{\partial x^4} + 2 \frac{\partial^4 w}{\partial x^2 \partial y^2} + \frac{\partial^4 w}{\partial y^4} \right) + \rho h \frac{\partial^2 w}{\partial t^2} = -p(x, y, t), \quad (1)$$

where  $\rho$  is the density of the plate,  $E$  is Young's modulus of elasticity,  $\nu$  is the Poisson ratio corresponding to the material of the plate and  $p$  is the applied external pressure.

A separable solution of the transverse modal displacement for a simply supported plate is of the form

$$w_{mn}(x, y, t) = \sum_{m=1}^{\infty} \sum_{n=1}^{\infty} W_{mn} \sin(k_m x) \sin(k_n y) e^{j\omega t} \quad (2)$$

where  $W_{mn}$  is the modal amplitude and  $m, n$  are the modal indices for modes along the  $x$  and  $y$  axes respectively. For boundary conditions of zero transverse displacement along the edges, the wavenumbers in each coordinate direction are

$$k_m = m\pi/a, \quad m = 1, 2, 3, \dots \quad k_n = n\pi/b, \quad n = 1, 2, 3, \dots \quad (3)$$

and the discrete frequencies at which the system resonates are given by

$$\omega_{mn} = \left( \frac{EI}{\rho h} \right)^{1/2} [k_m^2 + k_n^2]. \quad (4)$$

In the case of an actuator array, there are  $N$  point forces located at  $x_i, y_i$ , expressed through the function  $f_i(x, t) = F_i \delta(x - x_i) \delta(y - y_i) e^{j\omega t}$ . The resulting modal amplitudes are:

$$W_{mn} = \sum_{i=1}^N W_{mn}(i) = \frac{4}{M(\omega^2 - \omega_{mn}^2)} \sum_{i=1}^N F_i \sin k_m x_i \sin k_n y_i, \quad (5)$$

where  $M = \rho h a b$  is the total mass of the plate.

The solution stemming from Eqs. (2) and (5) is generally well-conditioned to determine the global system response. However, it is ill-conditioned for predicting near-field effects, as it does not model evanescent motions beyond a coincidence frequency, which is defined as:

$$f_c = \frac{c_0^2 \sqrt{3\rho_S/E}}{\pi/h}, \quad (6)$$

where  $c_0$  is the speed of sound in air and  $\rho_S$  is the density of the plate. This corresponds to the frequency at which the wavelength of the flexural waves on the plate is equal to the wavelength of the acoustic waves in air. A relatively high number of modes is also necessary to approximate the sum in Eq. (2) when it is truncated in the calculation of the model results. With both conditions met for the frequency range of interest, the solution of Eq. (5) is capable of reproducing both far and near-field effects [5].

## 2.2 Sound Radiation from a Vibrating Panel

The acoustic pressure in the far field, at a distance  $r$  from the defined centre point of the plate can be calculated using the Rayleigh integral in terms of the complex transverse velocities  $\dot{w}(\mathbf{r}_S)$  at points  $\mathbf{r}_S$  on the surface  $S$ , such that the pressure is given by

$$p(\mathbf{r}) = \int_S \frac{j\omega\rho_0 \dot{w}(\mathbf{r}_S) e^{-jkR}}{2\pi R} dS, \quad (7)$$

where  $R = |\mathbf{r} - \mathbf{r}_S|$ . This assumes that the plate is in an infinite baffle and thus only radiates into half-space. The complex velocity  $\dot{w}(\mathbf{r}_S)$  derived from Eqs. (2) and (5) is of the form

$$\dot{w}(\mathbf{r}_S) = \dot{W}_{mn} \sin\left(\frac{m\pi x}{a}\right) \sin\left(\frac{n\pi y}{b}\right) \quad \{0 \leq x \leq a\} \quad \{0 \leq y \leq b\}. \quad (8)$$

For  $N$  point forces acting at coordinates  $(x_i, y_i)$ , upon a plate, the total acoustic pressure at a point in the far field described by the coordinates  $(r, \theta, \phi)$  in the far field is expressed upon evaluation of the integral in Eq. (7) using the transverse modal displacement of Eq. (2). The infinite sum can be in practice truncated as the finite summation:

$$p(r, \theta, \phi) = \sum_{m=1}^{\infty} \sum_{n=1}^{\infty} \frac{j\omega\rho_0 e^{-jkr}}{2\pi r} \frac{ab}{mn\pi^2} \left[ \frac{(-1)^m e^{-j\alpha} - 1}{(\alpha/m\pi)^2 - 1} \right] \left[ \frac{(-1)^n e^{-j\beta} - 1}{(\beta/n\pi)^2 - 1} \right] \dot{W}_{mn}(i), \quad (9)$$

where  $\alpha = ka \sin \theta \cos \phi$  and  $\beta = kb \sin \theta \sin \phi$ . The above equation, in conjunction with Eq. (5), can be used to calculate the pressure radiated from the structural actuator array, provided a sufficient number of modes is considered and the frequency investigated is within the limit set by Eq. (6).

### 3. Parametric Study

The above mathematical model is used in a series of simulations towards a preliminary evaluation and optimisation of the structural array. For this study, the plate is considered as a 6082 aluminium alloy panel, a material that is relatively robust and lightweight. The thickness of the panel is fixed at 3 mm, which, in accordance with Eq. (6) gives the system a coincidence frequency of 4.1 kHz. Simulation results should, therefore, be reliable for frequencies below this threshold. Directivity control is implemented via the acoustic contrast maximisation process, described in the following section.

#### 3.1 Acoustic Contrast Maximisation

The directivity performance of any type of sound emitting system can be quantified by calculating the contrast between the average mean square pressure in two distinct zones defined as *bright* and *dark*, respectively referring to the regions where sound needs to be amplified or attenuated [7].

For an array of  $N$  elements with complex source strengths  $\mathbf{q}$  at a given frequency, the amplitudes of mean square pressure  $\mathbf{p}$  are given by vectors  $\mathbf{p}_B$  and  $\mathbf{p}_D$  for points in the bright and dark zones respectively. Given complex transfer responses between the sources and the pressure measurement points in the bright and dark zones,  $\mathbf{H}_B$  and  $\mathbf{H}_D$ , the acoustic contrast is defined at a given frequency as:

$$AC = \frac{\mathbf{p}_B^H \mathbf{p}_B}{\mathbf{p}_D^H \mathbf{p}_D} = \frac{\mathbf{q}^H \mathbf{H}_B^H \mathbf{H}_B \mathbf{q}}{\mathbf{q}^H \mathbf{H}_D^H \mathbf{H}_D \mathbf{q}} \quad (10)$$

where the  $^H$  superscript indicates the conjugate transpose of a respective vector or matrix.

Assuming that the system intended to radiate a directional sound field consists of a finite number of individual sources, the above relation allows for the formulation of a constrained optimisation problem [8]. With the introduction of the regularisation parameter  $\beta$ , the resulting Lagrangian can be shown to yield

$$\lambda \mathbf{q} = -[\mathbf{H}_B^H \mathbf{H}_B]^{-1} [\mathbf{H}_D^H \mathbf{H}_D \mathbf{q} + \beta \mathbf{I}] = \mathbf{M} \mathbf{q}. \quad (11)$$

The source strength vector  $\mathbf{q}$  that maximises acoustic contrast is proportional to the eigenvector of the matrix  $\mathbf{M}$  corresponding to its largest eigenvalue. Therefore, assigning these source strength values to the elements of the array achieves the highest level of acoustic contrast in the produced sound field possible for the system. In all subsequent simulations, the response is measured at points placed along a 2.8 m radius from the centre of the array in the forward half-space, and the coverage angle of the bright zone is set to 36 degrees.

### 3.2 Array Parameter Study

The first part of this parametric study regards the geometrical arrangement of the array of actuators used. For a fixed panel size of dimensions  $1\text{ m} \times 0.2\text{ m} \times 3\text{ mm}$ , simulations are run for different array layouts. The effects of actuator number on performance is evaluated by simulating arrays of four, five, and six actuators, with a fixed spacing of 14.3 cm between consecutive elements. Larger arrays are not considered, as the increased weight attached to the panel as well as the physical dimensions of the actuators compromise the validity of the mathematical model, but will also result in a less cost effective solution. Figure 2(a) shows the resulting acoustic contrast across frequency for these different array configurations. A higher number of actuators increases the value of contrast and also the effective bandwidth, with the lower frequency limit benefiting from a larger array.

The results stemming from changing the spacing between actuators are shown in Fig. 2(b), for an array of six actuators set at 7.1 cm, 10.7 cm, and 14.3 cm apart. The choice of spacings was made to avoid the coincidence of driving positions with zero displacement modal points on the panel. A longer array is again seen to improve the low frequency limit. The density and intensity of peaks at middle frequencies suggest that performance is affected by the activation of normal modes on the panel. Performance for all cases displays a cut off at roughly 1.8 kHz, though isolated peaks appear at some of the higher investigated frequencies. From these results a longer array demonstrates the best overall performance throughout a greater bandwidth.

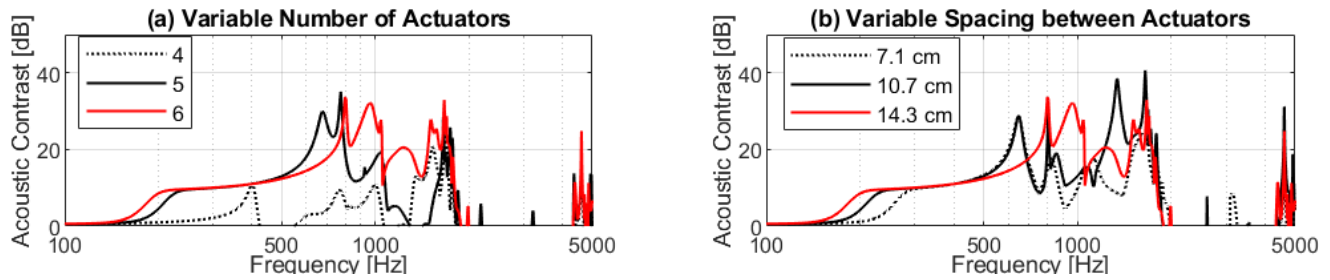


Figure 2: Acoustic contrast frequency response for structural actuator arrays of fixed panel size and variable array layouts, with (a) showing the effect of different numbers of actuators and (b) showing the effect of different spacings for a six actuator array.

### 3.3 Panel Parameter Study

In this section the effect of each panel dimension is individually investigated. The array used consists of six actuators and in all cases is centred on the panel. When evaluating different panel lengths, the actuators are spaced at 107 mm from each other, giving an effective array length of 535 mm. This serves to ensure a relatively good performance, whilst allowing for the testing of a broader range of panel lengths.

Figure 3(a) shows the acoustic contrast produced by the structural actuator arrays using different panel lengths. The low frequency limit improves by having a longer panel, as does the maximum value of contrast achieved. However, strong variations in contrast also appear due to the abundance of structural modes. The cut-off at 1.8 kHz persists in all cases, similarly to the previous part of this study.

Simulating structural actuator arrays with different panel widths allows for the maximum array length to be used, which has been shown to perform best, corresponding to six actuators 14.3 cm apart, with an overall length of 71.5 cm. The acoustic contrast frequency response when using panels of different width

is shown in Fig. 3(b). Low frequency response again benefits from a larger panel. The the maximum contrast achieved at middle frequencies appears to increase with a wider panel. The cut-off frequency which persisted in all previous cases changes here with the change of panel width; still, a clear trend that indicates the relationship between width and cut-off is not discernible.

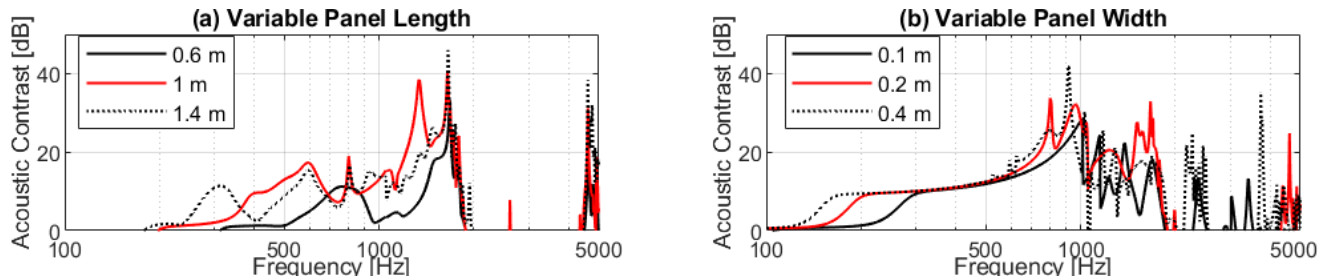


Figure 3: Acoustic contrast frequency response for structural actuator arrays of six actuators using different panel sizes.

### 3.4 Array Steerability

In many applications, it may be desirable to steer the directivity of the array. By re-assigning the defined bright zone and following the procedure presented in Section 3.1, the system can be controlled to direct the radiated sound field in specific direction. The simulated array comprises of six actuators, spaced at 143 mm from one another, and a  $1\text{ m} \times 0.2\text{ m} \times 3\text{ mm}$  panel.

Keeping the angle coverage fixed at 36 degrees, the direction of the bright zone is steered and the resulting acoustic contrast performance is displayed in Fig. 4. A significant increase in performance at the lower frequencies is observed as the beam approaches an angle of 90 degrees, with its response bearing similarities to that of an end-fire array (case of 72 degrees). In addition, positive contrast is also achieved at the higher investigated frequencies for the steered settings. This improvement, however, comes at the cost of reduced contrast at the mid-frequency range. Noteworthy in the case of the 54 degree steered setting as an exception to this trend, which shows a generally lower level of performance across the full bandwidth investigated. In a conventional loudspeaker array this would happen gradually as the angle shifted from 0 to 90 degrees, so in this instance, this response is thought to be due to antiresonance effects resulting from the vibration modes of the panel.

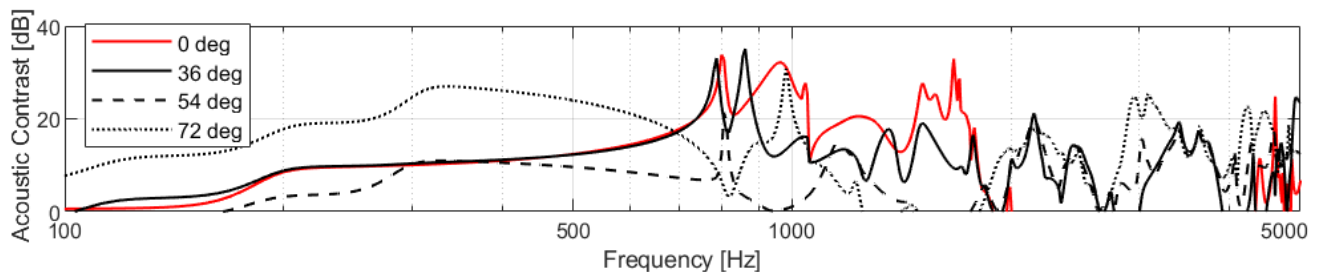


Figure 4: Acoustic contrast frequency response for a six actuator structural array under different directivity settings.



## 4. Experimental Validation

After conducting the simulation-based preliminary study, a prototype array has been constructed for the experimental validation of the structural actuator array. This prototype is depicted in Fig. 5(a), and consists of a rectangular aluminium 6082 panel, with dimensions of  $1\text{ m} \times 0.2\text{ m} \times 3\text{ mm}$ , six inertial actuators attached, and a wooden mounting apparatus. Measurements take place in an anechoic chamber; an array of eleven microphones placed along a half circle centred around the structural array, which corresponds to the same measurement positions as the simulations. Figure 5(b) depicts this arrangement, along with the designated bright zone, consisting of three microphones covering a 36 degree wide angle.

The responses from each actuator driven individually are used to construct the two transfer matrices,  $H_B$  and  $H_D$  of the system, which allow for the contrast optimisation process described in Section 3.1. A difference between the model and the experimental array is that, while in the former the values assigned to the actuators correspond to forces, while in the experimental implementation they are voltages. To ensure that the two systems are driven in a comparable fashion, regularisation is performed based on the normalised array effort for each case. This is the squared norm of source strengths, divided by the squared modulus of the strength of a single source generating the same on-axis pressure.

The resulting acoustic contrast response over frequency is shown in Fig. 5(c) for both the measurement and the equivalent simulation. From these results it can be seen that the simulations and experiments show a similar behaviour up to 1.8 kHz. The measured response does not follow the cut-off that characterised most simulations presented in the previous section, and instead drops to a relatively constant contrast of just under 10 dB at frequencies above 1.8 kHz. Additionally, the experiments show an improved performance at frequencies below 800 Hz, and conversely, a lower achieved contrast above the 1 kHz mark. These differences could be attributed to approximations in the model including the size and weight of the actuators. In reality, each actuator has a diameter of 25 mm, and the overall weight of the array attached to the panel amounts to 0.36 kg. Additionally, the wooden mounting apparatus used does not approximate the infinite baffle used in the simulations, influencing the radiated sound field.

Overall, the prototype array shows itself to be capable of a significant level of directivity. Particularly within the 200 Hz to 1.8 kHz range, the acoustic contrast is maintained above 10 dB. The disparity between the simulation and experimental results regarding the cut-off beyond 1.8 kHz indicates that the analytical model used has room for improvement. One step towards this direction is to include a more detailed modelling of the actuators and their driving forces.

## 5. Conclusions

This paper has investigated the potential for directivity control of a structural actuator array, a system comprising of an array of inertial actuators forcing the vibration of a panel, resulting in sound radiation. An analytical model was utilised in a series of simulations evaluating this concept. Controlling the directivity via the acoustic contrast maximisation method, results indicated a good performance within the 300 Hz to 1.8 kHz range.

Upon consideration of the results from the simulation-based parametric study, a prototype array was assembled employing six inertial actuators to drive a rectangular aluminium panel. This prototype was tested in terms of the degree of directivity it can achieve in an anechoic environment. The resulting frequency response generally falls in line with the simulations, however, for frequencies above 1.8 kHz the prototype that performs substantially better than predicted.

The results indicate that the analytical model is in need of refinement to improve its accuracy, especially at the higher frequency range. Nevertheless, the acoustic contrast performance of the prototype array shows promise for further development of the concept.

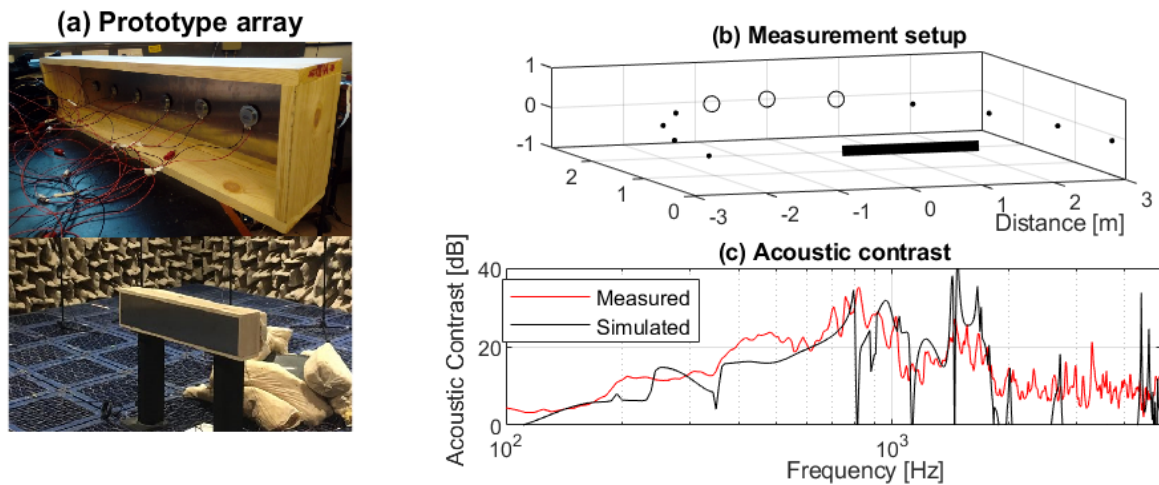


Figure 5: Prototype structural actuator array (a), measurement setup (b) and resulting acoustic contrast (c). In (b), the thick line notes the position of the array while the circles and dots, the position of bright and dark zone measurement points respectively. In (c), the resulting acoustic contrast is compared to that of an equivalent simulated array, using an array effort based regularisation.

## Acknowledgements

The authors gratefully acknowledge the European Commission for its support of the Marie Skłodowska Curie program through the ETN PBNv2 project (GA 721615).

## REFERENCES

1. Simón, M., Elliott, S. J. and Cheer, J. Loudspeaker arrays for family TV, *Proceedings of the 19<sup>th</sup> International Congress on Sound and Vibration*, Vilnius, Lithuania, 08–12 July, (2012).
2. Pondrom, P. Tschesche, J. Börs, J. and Melz, T. Loudspeaker array for the directional generation of acoustic warning signals of electric vehicles, *Proceedings of the 40<sup>th</sup> Annual Conference on Acoustics (DAGA)*, Oldenburg, Germany, 10–13 March, (2014).
3. Olszewski, D. Prasetyo, F. and Linhard, K. Steerable Highly Directional Audio Beam Loudspeaker, *Proceedings of the 9<sup>th</sup> European Conference on Speech Communication and Technology (Interspeech)*, Lisbon, Portugal, 4–8 September, (2005).
4. Rashedin, R. and Meydan, T. Sensors and Actuators A: Physical, *Journal of the Acoustical Society of America* **129** (1–2), 220–223, (2006).
5. Fuller, C. R., Elliot, S.J. and Nelson, P., *Active Control of Vibration*, Academic Press, London, UK (1996).
6. Cremer, L., Heckl M. and Petersson, B. A. T., *Structure-Borne Sound*, Springer-Verlag, Berlin-Heidelberg, Germany (1973).
7. Choi, J.-W. and Kim, Y.-H. Generation of an acoustically bright zone with an illuminated region using multiple sources, *Journal of the Acoustical Society of America* **111**, 1695–1700, (2002).
8. Elliott, S. J., Cheer, J., Choi, J. W., and Kim, Y. Robustness and regularization of personal audio systems, *IEEE Transactions on Audio, Speech, and Language Processing*, **20**(7), 2123–2133, (2012).